New Insights on Molybdenum Suboxide: Nature of Carbons in Isomerization Reactions

Enelio Torres-García,[†] Geonel Rodríguez-Gattorno,*[,†] Jorge A. Ascencio,[†] Laura O. Alemán-Vázquez,[†] José L. Cano-Domínguez,[†] Angel Martínez-Hernández,[‡] and Patricia Santiago-Jacinto[§]

Instituto Mexicano del Petróleo, Eje Lázaro Cárdenas 152, San Bartolo Atepehuacan 07730 México D.F. México, Universidad Autónoma Metropolitana, A.P. 55 534, 09340 México D.F., México, and Departamento de Materia Condensada, Instituto de Física, Universidad Nacional Autónoma de México, Coyoacán, 04510, México D.F., México

Received: May 19, 2005; In Final Form: June 28, 2005

MoO_3 transformations under isomerization process conditions were studied. The products obtained after different times under stream (H_2/*n*-heptane mixture, 18.5 bar, at 370 °C) were characterized by X-ray diffraction, Raman spectroscopy, thermal analysis, and high-resolution transmission electron microscopy (HRTEM). Theoretical quantum calculations were carried out with the aim of understanding the paradox of the real active phase in isomerization reactions. Theoretical calculations predict the existence of a metallic-like MoO phase with a structure that matches the X-ray diffraction experimental results. From experimental and simulated HRTEM images it was possible to identify the presence of small MoO cubic crystallites inside MoOx matrix phases. These results also support the previously proposed idea that isomerization reactions take place as a result of the existence of a bifunctional catalyst. The Raman and thermo-programmed oxidation (TPO) analyses show the existence of at least two types of carbonaceous deposits which tend to increase its ordering with the increase of time under stream. The carbon K edge in electron energy loss spectroscopy (EELS) of a sample after 24 h under stream shows that these carbonaceous deposits consist of a mixture of sp^2- and sp^3-hybridized carbons.

Introduction

Molybdenum oxide is one of the few oxides with many applications as a catalyst. In recent years MoO_3 has been shown to be a very efficient catalyst (high conversion rates and high selectivity) in isomerization reactions. The importance of catalytic isomerization reactions is based on the increase in the octane number in gasoline. In a typical catalyzed isomerization process the MoO_3 catalyst is exposed to hydrogen gas and a complex mixture of hydrocarbons. Most of the basic studies to elucidate mechanisms and active phases use a H_2/model-alcane (e.g., butane, hexane, heptane)[1,2] mixture. When MoO_3 is used as a catalyst, hydrogen partially reduces the oxide and hydrocarbons chemisorb dissociatively at the catalyst surface, thus provoking complex reactions that are an important source of carbons incorporated in the catalyst. Despite the ample experimental studies on the MoO_3 catalyst, investigations on the nature of surface-deposited carbons in MoO_3 during catalyzed processes are usually ignored. Hence, an understanding of the nature of carbon is a very important step toward the catalyst recovering or its activation process. Since it is a special characteristic of carbon chemistry that different carbon modifications cannot be obtained as pure-phase material, various types of carbons usually can be found in catalytic conditions. The role of carbon in heterogeneous catalysis could be multiple; sometimes it becomes a poisonous material, and in other cases it enhances the activity and selectivity of the catalyst.[3−5]

There are many controversial questions in the literature concerning catalytic systems based on MoO_3[6,7] which still remain unanswered. Molybdenum oxycarbide is supposed to be the active phase in isomerization processes. The most intensive studies on the structural aspects concerning the believed catalytically active phase (namely, MoOxCy) corresponds to Ledoux's group.[8−10] On the basis of some experimental facts Ledoux and collaborators proposed the existence of a molybdenum oxycarbide with a cubic fcc structure (a = 4.1 Å), which is formed under H_2/alkane mixture at 350 °C. In contrast, Matsuda[11−13] points out the existence of an active phase based on a molybdenum suboxide with composition similar to that of MoO. On the other hand, Wang et al.[14] obtained the same cubic phase (with Mo/O ratio near to 1, having a cubic cell parameter a = 4.08 Å) under TEM conditions (high vacuum, electron irradiation, and avoiding interaction with carbon). In this case, the cubic MoO forms a small cluster inside the MoO_3 matrix.

It is not well understood if molybdenum oxycarbide forms a true bulk phase or if it is a simple interface between partially reduced molybdenum oxide and a carbon type in which carbon bonds to open valences of this metal (dangling bonds) on the surface.

The present paper is devoted to elucidating a more realistic and general chemical approach to MoO_3 catalyst behavior in the isomerization process. Because hydrocarbon conversion reactions appear to occur in the presence of a carbonaceous layer, the study of this layer has been explored, trying to understand the MoO_3 behavior in catalysis. According to our experimental results, the MoO_3 catalyst should be viewed as a rather complex system in which not only molybdenum suboxides

* To whom correspondence should be addressed. Phone: 52-771-7170616. Fax: 52-771-7163059. E-mail: geonelr@imp.mx.
[†] Instituto Mexicano del Petróleo.
[‡] Universidad Autónoma Metropolitana.
[§] Universidad Nacional Autónoma de México.

10.1021/jp052633b CCC: $30.25
Published on Web 08/27/2005

are present but also different types of carbons (ordered and disordered) that could play a very important role in the catalysis of isomerization reactions. Due to this complexity, theoretical quantum calculations were accomplished in order to clarify some important aspects of the molybdenum chemistry and see how the atomistic order affects the electronic structure and the corresponding physicochemical properties. The results predict the existence of a stable MoO cubic phase that is distinguished by having a metal-like behavior that could explain the generalized chemical behavior of molybdenum in catalytic systems.

Experimental Section

Sample and Methodology. Molybdenum oxide carbide was obtained directly from the oxide MoO_3 (99.5%, Fermont) with a 20 μm particle size and surface area less that 1.0 m^2/g. The solid (1 g) was placed in a continuous flow stainless steel reactor (0.9 cm in diameter), and the temperature was raised to 643 K under hydrogen flow. The pressure was kept at 18.5 bar. Afterward, *n*-heptane (99% purity) was continuously fed (using an LDC analytical minipump) to the reactor at a rate of 5 mL/h. The hydrogen flow was controlled with a Brooks 5850E mass flow controller to keep a H_2/n-C_7 molar flow ratio of 39/1. The samples subjected to different reaction times (4, 12, 24, and 30 h) were studied by different characterization techniques.

Surface area measurements of the samples were performed in a Micromeritics ASAP system, and the particle size was determined by the ASTM D-4464-00 method (standard test method for particle size distribution of catalytic material by laser light scattering).

Samples were characterized by X-ray diffraction using a Siemens diffractometer (model D5000) with Cu Kα radiation and a Ni filter. The operating conditions were 30 kV and 20 mA in the angular range 4−70° in 2θ. Crystalline phase identification based on XRD patterns was aided by the ICDD-PDF-2 database.

The Raman spectra were recorded at room temperature using an Yvon Jobin Horiba (T64000) spectrometer equipped with a confocal microscope (Olympus, BX41) with a laser 514.5 nm at a power level of 10 mW. The spectrometer is equipped with a CCD detector, which is Peltier-cooled to 243 K to reduce thermal noise.

For HRTEM study the samples were dispersed in ethanol, and a drop of the suspension was then placed in a holey carbon Cu grid. The observations were made with a JEOL 2010F transmission electron microscope equipped with a Gatan 666 parallel spectrometer. Attention was particularly focused on the C K-edge transition region around 300 eV.

For temperature-programmed oxidation (TPO) a 50 mg of sample was used. A flow of 25 cm^3/min of a mixture of 5% of O_2 in an Ar balance was used to oxidize the carbonaceous deposits, raising the reactor temperature from room temperature to 800 °C at 8 °C/min. The combustion products were monitored with a dynamic sampling mass spectrometer (HIDEN, HAL RC 301) simultaneously measuring the mass/charge signals 32 and 44, corresponding to O_2 and CO_2, respectively.

Structural analyses were supported theoretically by means of ab initio quantum mechanic electronic analysis for the MoOx and MoOxCy systems. Calculations were based on a wave-plane method and on density functional theory (DFT) using the corrected gradient approximation and the Perdew−Burke−Ernzerhof functional (PBE)[15] with an energy cutoff of 380 eV and a 6 × 6 × 6 equivalent *k*-point set that corresponded to an ultrafine level of theory using the CASTEP software[16] as part of Cerius by Accelrys. Density of states was calculated for each model with a particular separation between neighboring *k*-points in the Monkhorst−Pack grid of 0.04 1/Å.

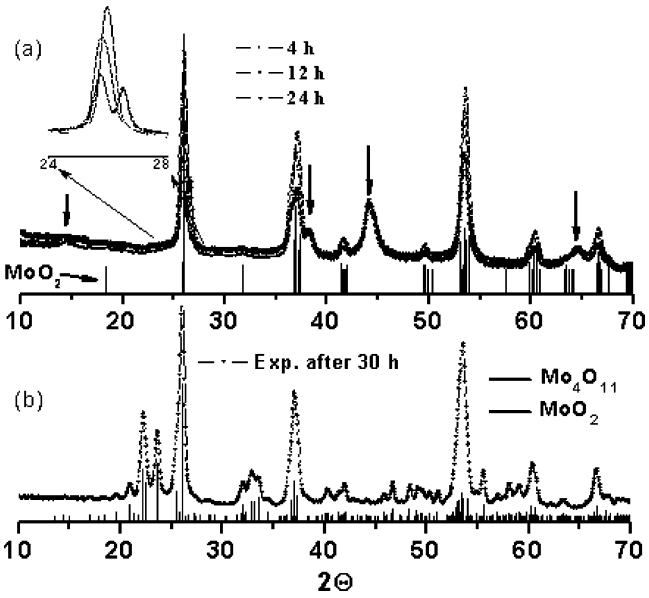

Figure 1. (a) Time evolution of carbon-modified MoO_3 after 4, 12, and 24 h under stream. For comparison, the XRD pattern for MoO_2 (JCPDS data file no. 32−671) is also shown. The insert plot is enlarged for better clarity. Arrows indicate reflections that are usually assigned to MoOxCy. (b) XRD patterns for carbon modified MoO_3 after 30 h and the corresponding XRD pattern of MoO_2 and Mo_4O_{11}.

Results and Discussion

An important feature of the isomerization experiments is the fact that in order to obtain significant conversion rates MoO_3 should be initially reduced before adding the alkane, suggesting requiring the presence of a reduced oxide phase to guarantee good catalyst performance. Similar behavior has been previously reported by Ledoux et al.[17] and also by Matsuda's group.[11−13] According to our results[18] the conversion rate reaches a maximum between 12 and 24 h that slightly declines to a steady state after 30 h.

Specific Area. BET surface area measurements showed that the specific area of the starting MoO_3 sample is less than 1.0 m^2/g. The surface areas of "carbon-modified MoO_3" samples increased as a function of reaction time between 50 and 140 m^2/g, which suggests that the specific area increases during reduction of MoO_3. Although this result has been extensively discussed in the literature, it is still not fully understood and its relationship with catalytic activity remains unclear. In our opinion it should be stated that there are two main sources that provoke this surface area increase, one being the collapse of MoO_3-elongated crystals into surface-fractured material with a high concentration of voids formed from starlike cracks due to the phase change and lattice contraction produced upon reduction of MoO_3 to MoO_2;[18−20] the other important source is the carbon types and their content at the surface of the catalyst. This must be taken into account for interpretation of surface area modifications in catalysis processes that involve organic molecules. In general, since carbons produced during catalytic processes have a very high surface area, small quantities of carbon imply a substantial increase in system surface.[3] In this case, those types of carbons that deposit as carbonaceous not participating in a Mo−C bond are referred to.

X-ray Diffraction. XRD patterns of the carbon-modified MoO_3 obtained by reduction with a mixture of H_2/n-C_7 at 370 °C for different times are given in Figure 1. For the starting

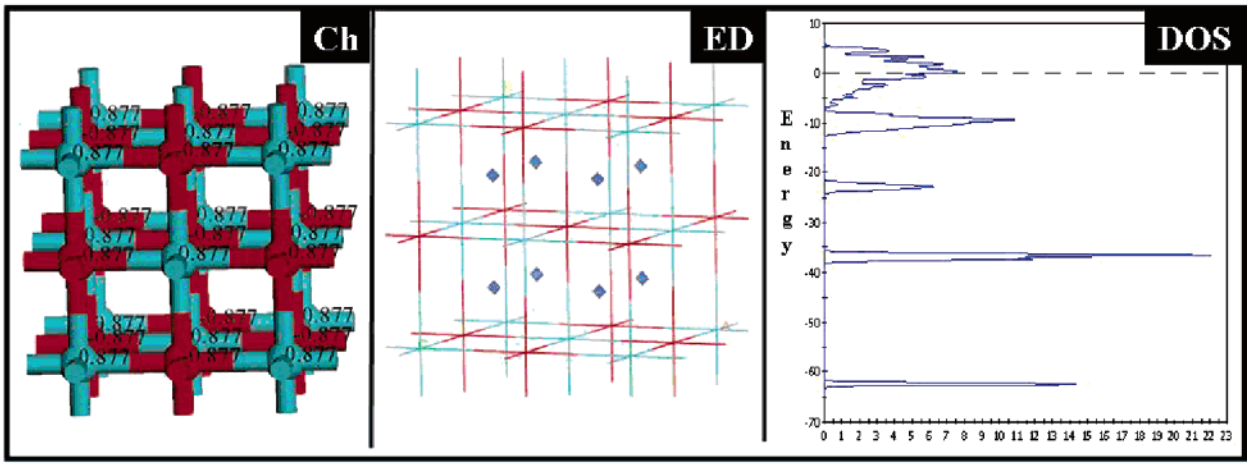

Figure 2. Obtained relative charge (Ch), electron density isosurface (ED), and density of states (DOS) of the MoO cubic crystal obtained from theoretical quantum calculations.

MoO_3 the XRD pattern (not presented here) shows a narrow diffraction line corresponding to MoO_3 (JCPDS data file no. 05-0508). After 4, 12, and 24 h under flow of the H_2/n-C_7 mixture the X-ray diagram (see Figure 1a) can be essentially attributed to the presence of MoO_2 (JCPDS data file no. 32-671). In addition, other reflections with interplanar distances of 6.1, 2.346, 2.04, and 1.44 Å can be observed. Ledoux et al. associated these reflections with molybdenum oxycarbide. These peaks are assumed reflections from a MoOxCy structure belonging to a fcc framework with a cell parameter of 4.1 Å, their conclusion being based on a combination of simulations of powder XRD and microdiffraction performed with a transmission electron microscope (TEM). However, more recently Wang et al.[14] demonstrated that in TEM conditions (high vacuum and electron irradiation, avoiding interaction with carbon) MoO_3 undergoes a structural transformation leading to a molybdenum suboxide with a rock-salt (fcc) crystal structure having an experimental cubic parameter $a = 4.08$ Å. This value is the same as that reported by Ledoux within experimental error of the two techniques. Despite the greatly different conditions for MoO_3 reduction, both groups reach the same conclusions from a structural point of view. Obviously, this is not a casual coincidence; undoubtedly, in both cases there is the same product having discrepancy only in their respective proposed composition.

The low-intensity peak at $d_{hkl} = 6.1$ Å, which can be assigned to neither of the molybdenum oxides nor MoOxCy as proposed by Ledoux et al., could correspond to the most intense reflection line (1,0,−1) of residues of hydrogen molybdenum oxide hydrate (JCPDS data file no. 41-0060). For the sample after 24 h there is also a peak at 3.35 Å (see insert in Figure 1a) which can be assigned only to the main reflection from the 002 interplanar distance in graphite-like carbonaceous deposits; however, this reflection is not present for the sample after 30 h, thus suggesting that this carbon is consumed in isomerization or collateral reactions.

On the other hand, the XRD diagram for the sample after 30 h under stream (Figure 1b) shows that the sample is composed of a mixture of Mo_4O_{11} (JCPDS data file no.73-1538) and MoO_2, and no other peaks can be detected in this case. Mo_4O_{11} is a well-known phase[6,7] obtained during the reduction of the MoO_3.

Another crucial feature of XRD results is that at 30 h under stream the supposed active catalyst (molybdenum oxide carbide) cannot be observed in the XRD pattern (Figure 1b); however, by this time the catalyst has reached a steady state in the conversion, which implies that the cubic phase formed during the first reaction stages is not necessarily the active phase. This experimental evidence appears to refute the established idea that the active catalyst phase is bulk molybdenum oxycarbide. It implies that the cubic phase is not necessarily the only phase contributing to the activity of the catalyst; therefore, for longer reaction times (e.g., 30 h) the isomerization reaction is supported by the activity of the residual MoO_2, as demonstrated by Katrig et al.[21] The absence of the cubic phase could explain why the activity decreases after 24 h. Consequently, we prefer to see the system as a complex mixture of molybdenum oxides in addition to those disordered and ordered carbons (usually classified as carbonaceous deposits) in which different active phases could be contributing to the total activity of the catalyst.

However, the fact that other authors demonstrated that the MoO_2 phase is very ineffective toward selective isomerization cannot be discarded; hence, one plausible explanation for the steady state at longer times can be found in the small quantities of the active phase (MoO) that remains in the sample, as was proposed previously by Wehrer et al.[22]

For the purpose of clarifying which one of the two cubic phases is most probably present during the reduction of MoO_3, several ab initio quantum mechanical geometry optimizations were carried out with the DFT-based calculation and with the $6 \times 6 \times 6$ k-point basis set, i.e., at the ultrafine level of theory, for the MoO and MoOC systems. According to the calculated values of the formation enthalpy, high stability is expected in these systems, which predicts the existence of both phases; however, in addition to small deformations from the cubic periodicity in the model, the calculated cell parameter for the MoOC system differs considerably ($a = 4.34$ Å, see Supporting Information) from the experimental values ($a = 4.08$ Å), while those calculated for MoO match the experimental observation. This result appears to favor the proposal of Wang et al., which implies that during catalytic processes the formed cubic phase corresponds to a molybdenum oxide rather than to a molybdenum oxycarbide. In fact, the presence of carbon substituting oxygen in the cell appears to relax the fcc parameter to higher values, resembling more a molybdenum carbide structure[23] than the so-called molybdenum oxycarbide.

The predicted relative charge (Ch), electron density isosurface (ED), and density of states (DOS) of the MoO fcc crystal model are given in Figure 2. The results show a homogeneous relative charge distribution between Mo and O. The absolute charge

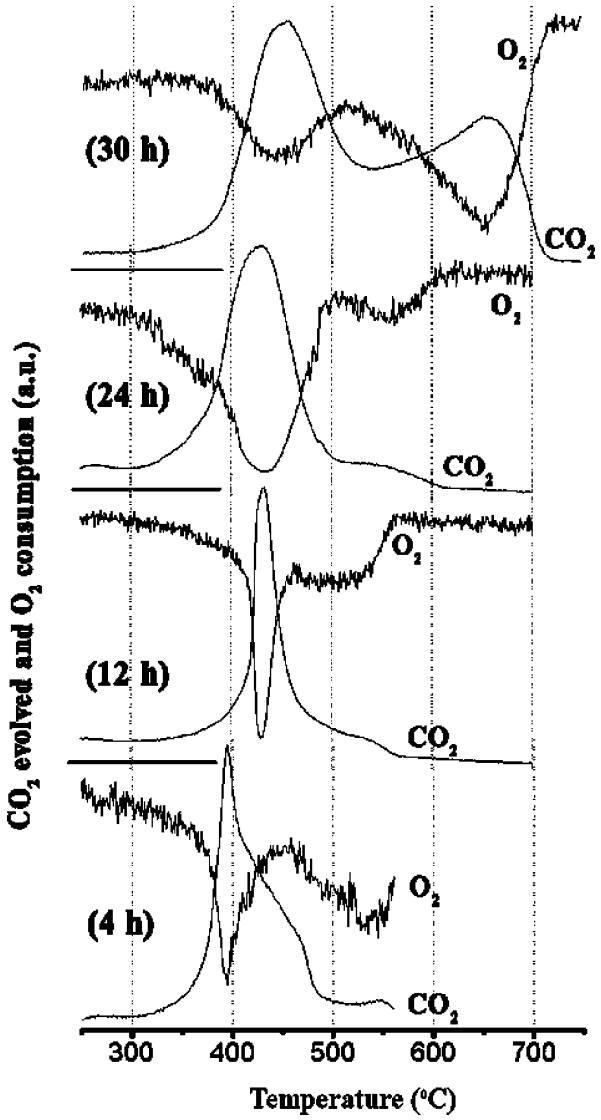

Figure 3. Thermo-programmed (TPO) oxidation curves for samples after 4, 12, 24, and 30 h under stream.

(0.877 positive for Mo and negative for O) generates a uniform electron density having practically no evident electrostatic potential; however, the corresponding DOS establishes that this crystal has metallic-like behavior with a large number of plausible conductive electrons, which implies no gap similar to metals. It must be noticed that this identified effect for MoO implies a significant difference for a catalyst material, since small aggregates of this phase must produce similar activity on metallic clusters such as Pt and Pd.

This type of material induces important modifications on carbon products, as observed for metallic clusters.[24,25] The aggregation and production of fullerene and nanotubes as produced by these kinds of clusters[26] has been well studied. The predicted metallic behavior in this kind of molybdenum compound is a novel property that could explain the high performance of the molybdenum oxides as catalyst under reducing conditions.

TPO-MS Analysis. A temperature-programmed oxidation (TPO) with a mass spectrometer (MS) was used to follow the product gases (O_2 consumption and evolved CO_2) during the course of the oxidation process of carbon-modified MoO_3 (Figure 3). It is common to find various and simultaneous events in thermal analyses of the carbon-modified MoO_3 system (obtained under the present conditions).[27] Observation of the different events is largely influenced by the conditions of the reaction, surface morphology, and MoO_3 particle size.[18,27]

It can be observed that at least two thermal events are clearly defined, each one related to oxygen uptake throughout oxidation of either MoO_{3-x} or carbon according to the following equations

$$MoO_{x(s)} + (3 - x)/2O_{2(g)} \rightarrow MoO_{3(s)} \quad \text{(I)}$$

$$C^{i}_{(s)} + O_2 \rightarrow CO_{2(g)} \quad \text{(II)}$$

where MoO_x and C^i denote a molybdenum suboxide and one of the possible carbon types formed during catalytic reactions, both processes being simultaneous at some stages.

The first carbonaceous material starts to oxidize at temperatures around 330 °C with a narrow temperature profile. The second carbon oxidizes at temperatures over 500 °C, covering a wider range of temperatures, its contents tending to increase with sample time under stream. Oxidation of carbon is a complex gas−solid reaction which is strongly influenced by its defect structure, diffusion of reactants and products, and oxygen chemical potential among other variables. Therefore, the different steps in TPO curves under the same conditions are a clear indication of the different nature of carbons present in the samples. It interesting to note that the start of carbon oxidation (first step) occurs at temperatures that are very low for known carbons, even for those known as active carbons black,[3] which is an indication of the high reactivity of this type of carbon formed in the catalyzed isomerization process.

Raman Spectroscopy. It is well known that Raman spectroscopy provides important information on the carbon structure. The bands corresponding to MoO_3 and its reduced oxides have been thoroughly studied previously.[28−30] Therefore, we focus our attention on the main frequency range corresponding to carbonaceous Raman response. In addition to MoO_3, MoO_2, and Mo_4O_{11}, the presence of carbonaceous product was detected in the samples. The signals are particularly intense on particles of small size and with a low degree of preferential growth. For the sample after 4 h the carbon Raman signals are very weak, although a small band can be detected around 1600 cm^{-1}. Figure 4 shows the Raman spectrum for the samples 4, 12, 24, and 30 h, respectively. There are two broad peaks at around 1600 and 1380 cm^{-1}. The first at 1610 cm^{-1} is attributed to the stretching mode of the individual sheets in graphite (E_{2g} mode, the so-called G band of graphite), and the other around 1380 cm^{-1} is assigned to an A_{1g}-type mode called the disorder ("D" band) band. The appearance of these two peaks is in agreement with the finite size of the graphite particles; however, it is interesting to note that carbonaceous materials start to deposit as organized carbon (D band absent for 4 h) in the first stages of the isomerization process.

The semiempirical relation developed by Knight and White,[31] who found that the in-plane crystallite dimension (La) is an approximately linear function of the ratio of the integrated spectral peak intensities (I_G/I_D), has been applied to a wide range of carbon materials including pyrolytic, glassy, amorphous, and crystalline graphite.

Using this empirical formula ($La = 4.4I_{1600}/I_{1380}$), where I_{1600} and I_{1380} are the intensities of peaks corresponding to the E_{2g} and A_{1g} modes, respectively, La (the in-plane carbon particle diameter) was estimated to be 2.5, 3.1, and 8.4 nm for samples at 12, 24, and 30 h under stream (inserted plot on the right in Figure 4). This behavior indicates an increase of the carbon order along the increase of the sample time under stream. Tysoe and Barlett[32] found a similar behavior in their study of the carbonaceous deposits on the MoO_3 catalyst applied to propylene

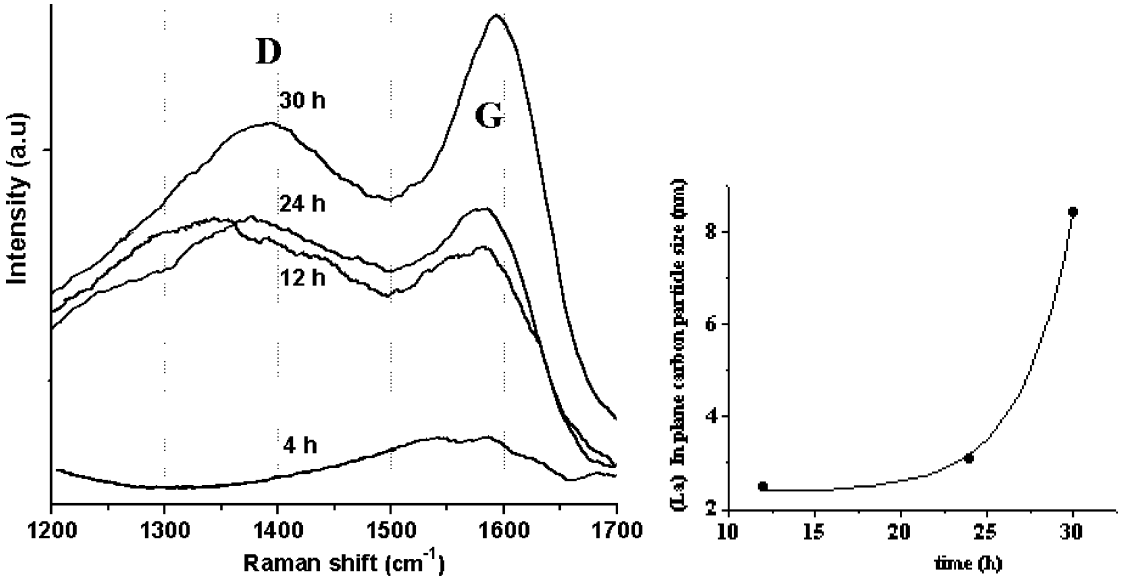

Figure 4. Raman spectra of samples after 4, 12, 24, and 30 h under stream. The plot on the right corresponds to the calculated in-plane carbon size (La) obtained from the integral area of G and D bands.

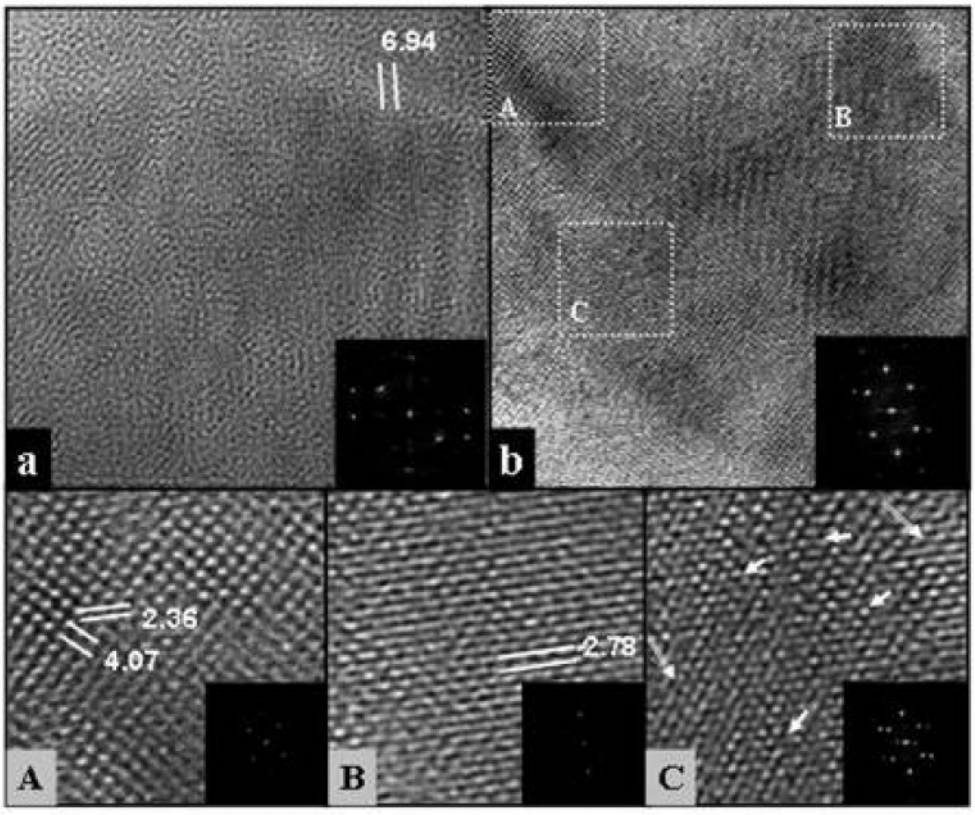

Figure 5. HRTEM micrographs of representative zones in MoO_3 samples after 24 h of reaction at 370 °C under $H_2/n\text{-}C_7$.

metathesis. In addition, it is interesting to note that carbonaceous material starts to deposit in the first stages of the reaction as an ordered carbon (D band is absent), indicating the uni- or bidimensional character of this carbon.[33]

According to our TPO-MS and Raman results, it can be stated that there is a mixture of different proportions of carbonaceous materials with different range of order. Both techniques reveal that the carbons tend to organize and grow under stream, becoming less reactive.

HRTEM. Using the simulated images (shown in Supporting Information) the samples seem to be composed of multiple phases of molybdenum oxides; however, the presence of the fcc phase is also demonstrated, and it is found embedded in the sample as small aggregates. In Figure 5 HRTEM micrographs show two different types of contrast observed on the sample. For most of the observed zones layerlike contrast can be found (as in Figure 5a) with measured distances that match multiples of (020) planes of MoO_3. In addition, (mainly in the borders of the particles) images that are composed of several types of contrasts are also observed. The small grains are immersed in bigger domains, as shown in Figure 5b. From selected regions (7.5 nm × 7.5 nm) of this image evidence of square dots arrays (Figure 5A) with distances (in angstroms) that match the fcc MoO phase (001 and 011 planar distances)

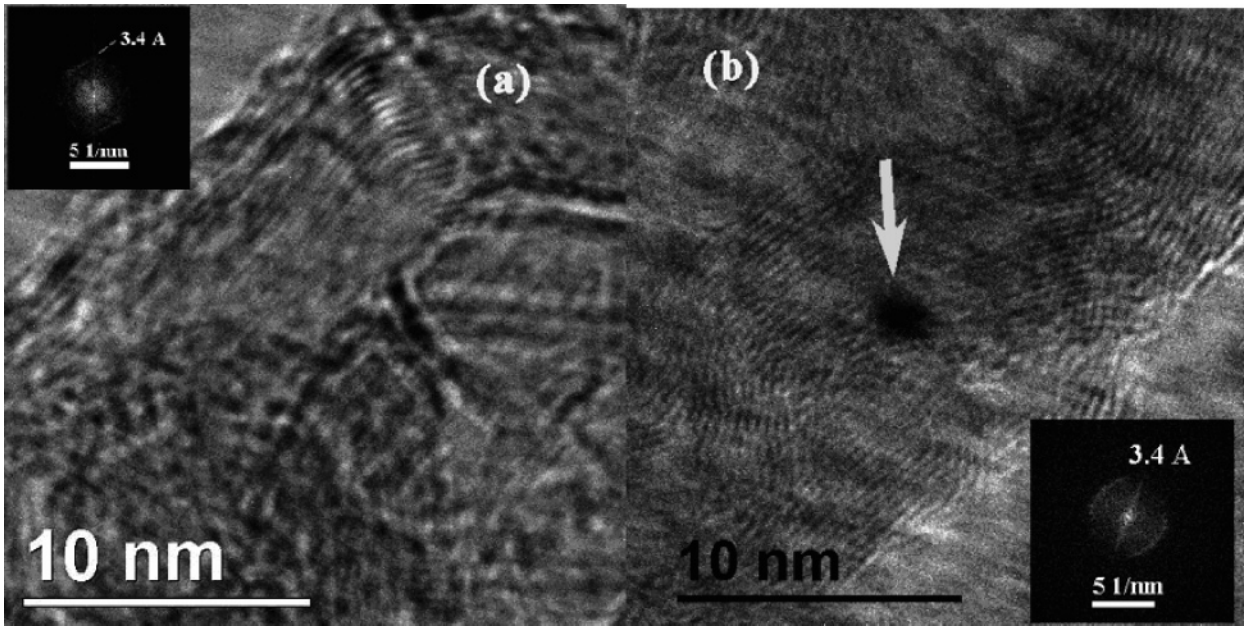

Figure 6. HRTEM micrographs of representative zones in MoO_3 samples after 30 h of reaction at 370 °C under $H_2/n\text{-}C_7$.

can be identified. Layered contrast with planar distances corresponding to the MoO_3 phase and a region where it is possible to identify multiple defects (shown by single line arrows) and a well-ordered section (denoted by double line arrows) are shown in Figure 5B and C, respectively.

It is important to note that while the fcc-like arrays are observed as clusters with a radius of at least 5 nm, the orthorhombic phase in which these clusters are embedded is much bigger. This kind of contrast is observed in the production of small grains to release strain in irradiated,[34] mechanically produced,[35] and even chemically synthesized nanostructures[36] where the expended energy in its production generates an excessive strain inducing a cluster formation of a different phase as independent aggregates. In fact, the C-selected area in Figure 5 shows an apparent reconstruction of the sample structure induced by defects, producing small regions with a disordered-like contrast. The formation of this kind of cluster with metallic characteristics (according to theoretical quantum calculations) inside a matrix of other molybdenum oxides (with more acidic character as in MoO_3 or MoO_2) creates an ideal situation for a catalyst that plays the role of a bifunctional material, especially in reactions that demand both kinds of sites.

This could have a very important connotation for the mechanism formulation in the Mo−O catalyst. In the case of catalyzed isomerization reactions there is contradictory information about the mechanism. Ledoux et al. proposed a bond-shift mechanism involving metallocyclic intermediates, while Katrib and co-workers[37,38] and Matsuda et al. proposed that isomerization proceeded via the conventional bifunctional mechanism as in Pt/zeolite systems. Our experimental and theoretical results suggest that the Mo−O system is expected to behave basically as a Lewis-acid−metallic catalyst, which supports the idea of a bifunctional mechanism.

To distinguish the effect and catalytic behavior of these fcc-like clusters, HREM image analysis was also focused on the carbon deposited on the MoOx materials, and evidence of the graphene materials is clearly identified in many sites of the sample.

In Figure 6 there can be recognized a common contrast and lattice spacing corresponding to graphite-like and structures derived from it, which is on the surface of the MoOx matrix. Deposited carbonaceous material tends to form bundle-like shapes with a thickness between 6 and 10 nm. The distance $d = 3.4\ (\pm\ 0.05)$ Å matches the typical interlayer distance in carbon structures formed by staked graphenes. These dimensions are in accord with those obtained by Raman spectroscopy. Of particular interest is the fact that the fringe contrast is over and around a molybdenum oxide nanoparticle of a 2.1 nm radius, which is notably isolated from other morphologies and the MoOx matrix. This image is commonly observed for the growing process studies of carbon nanotubes and onion-like carbon nanostructures, where the presence of metallic nanoparticles is well identified as precursors of the growing phenomena. Similarly, in Figure 6b there can follow an effect of the presence of this cluster which must be an fcc-like structure. In fact, analysis of fringes direction clearly denotes that the graphene material is dominated by the presence of this particle because even the curved fringes tend to be originated or directed to the darker cluster (marked with an arrow). The physicochemical implications of the presence of a metallic-like electronic structure in a molybdenum oxide phase are based on the possibility that this FCC-like array dominates the carbon generation process that has been previously assigned to the molybdenum oxide carbide. In this way, the FCC-like clusters of MoO must contribute significantly to the catalytic process because of their metallic behavior.

Electron Energy-Loss Spectroscopy. Electron energy-loss spectroscopy (EELS) studies are useful to distinguish between different carbon structures. It is a method which is directly related to the primary process of electron excitation. A beam of electrons will lose a certain amount of kinetic energy by Coulomb repulsion with inner- (high loss) or outer- (low loss) shell atomic electrons of the target compound. There is an inelastic scattering for the transmitted electrons as a consequence of the repulsion. The scattered intensity is recorded as a function of the decrease in kinetic energy.[39] Figure 7 shows the EELS spectrum of the O K edge and the Mo M3 edge of a sample subjected to 24 h under stream; this is considered the most representative from a catalytic point of view. By this time the catalyst sample has reached a steady state with a maximum in the conversion.[18] For Mo oxides, O has its K edge with a threshold around 526 eV and Mo the M3 edge at about 391

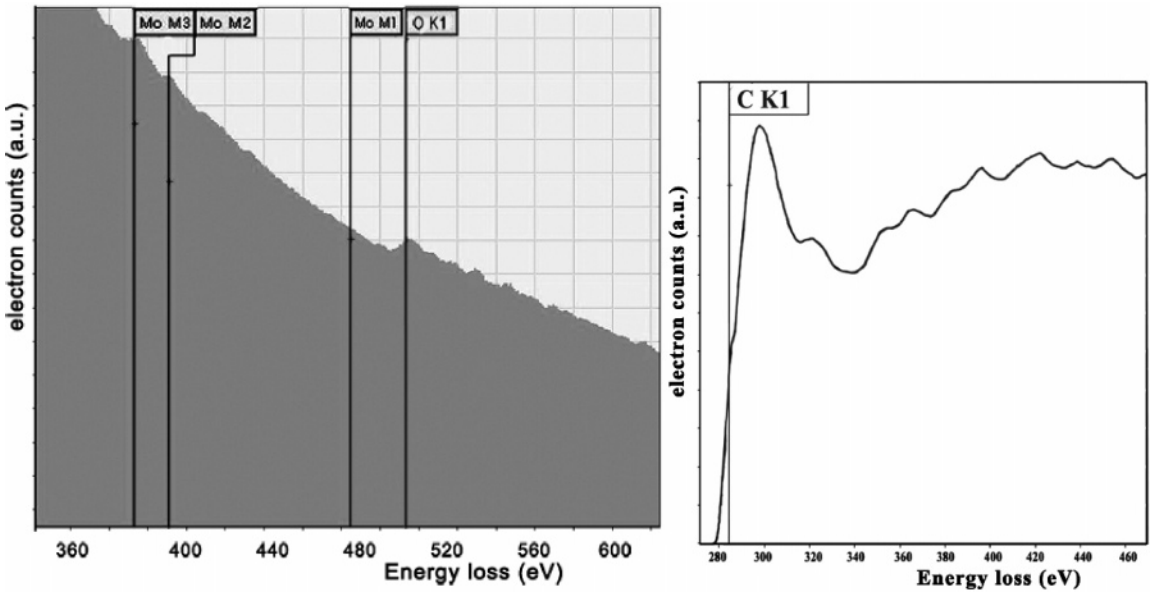

Figure 7. EEL spectra containing both the O *K* edge and the Mo *M*3 edge of a MoO_3 sample after 24 h under stream. (right) Enlarged EELS C K edge (275−460 eV) in the same sample.

eV. The less distinguishable shoulder at about 540 eV is associated to a molybdenum oxide with composition near MoO.[14] On the right of Figure 7 the carbon K edge enlarged. The peak shape structure near the ionization edge does not fit graphite, diamond, or pure molybdenum carbide;[40] it resembles the amorphous carbon spectra more than other kinds of carbons, although it is probably a result of various types of carbons (i.e., diamond-like, amorphous).[39]

For instance, there is an almost imperceptible shoulder at 285.5 eV that corresponds to the sharp peak at the absorption edge of the excitation of the carbon K-shell electron (1s electron) to the empty antibonding π^* orbital, which is expected for graphite and carbide materials. Its low intensity reveals that the sp^2/sp^3 bonding proportion is small (the unoccupied electronic states differ markedly for sp^2- and sp^3-hybridized carbon), which agrees with the presence of a peak at 325 eV that is expected for diamond-like carbons (sp^3-hybridized carbon).

Finally, as a summary of the experimental results it can be stated that the activity of the MoO_3 catalyst appears to be modulated by the presence of different phases, which contributes to the total activity of the system. For instance, the presence of MoO cubic is probably the reason for the enhanced activity at the first reaction stages. According to theoretical calculations the presence of this phase could increase the density of metallic sites necessary for catalysis. The absence of this phase combined with the increasing carbonaceous content (at catalyst surface) should be responsible for the decreases in activity for longer reaction times.

Conclusions

The following conclusions were drawn from the present study. According to X-ray diffraction analysis, structural changes in MoO_3 do not support the idea that molybdenum oxycarbide is the active phase for isomerization reactions. The theoretical calculations predict the existence of a metallic-like MoO phase with a structure that matches the X-ray diffraction and HRTEM experimental results. This is a novel property that supports the proposed idea that isomerization reactions take place via the existence of a bifunctional catalyst and refutes the established idea concerning the existence of an active MoOxCy catalyst. The thermal profile obtained from TPO-MS during the oxidation process reveals the strong influence of the reaction time on the chemical nature and composition of the residual carbonaceous deposits. As catalytic reactions proceed, the carbonaceous matter appears to be more ordered and less reactive. This is also supported by the Raman and HRTEM observations. The presence of different carbon types on the surface of the catalyst is a fact that must be taken into account for interpretation of surface area modifications in catalysis processes. The carbon K edge in EELS of a sample at 24 h after under stream shows that most of these carbonaceous deposits consist of a mixture of sp^2- and sp^3-hybridized carbons. From experimental and theoretical results, Mo−O system can be idealized as a perfect bifunctional catalyst in which metallic clusters form a kind of composite along the Lewis-acid MoO_x ($x \geq 2$) oxide matrix. Its presence could explain the enhanced activity at the first stages of the isomerization reaction.

Acknowledgment. L.O.A.-V. thanks the Mexican Oil Institute for financial support (Project D-0280). G.R.-G. is grateful for postdoctoral financial support from the Mexican Oil Institute.

Supporting Information Available: Calculated model cell parameters for the MoOC system and HRTEM-simulated images for MoO fcc model. This material is available free of charge via the Internet at http://pubs.acs.org.

References and Notes

(1) Del Gallo, P.; Meunier, F.; Pham-Huu, C.; Crouzet, C.; Ledoux, M. J. *Ind. Eng. Chem. Res.* **1997**, *36*, 4166.

(2) Blekkan, E. A.; Pham-Huu, C.; Ledoux, M. J.; Guillet, J. *Ind. Eng. Chem. Res.* **1994**, *33*, 1657.

(3) Schlögl, R. Carbons. In *Preparation of Solid Catalysts*; Ertl, G., Knözinger, H., Weitkamp, J., Eds.; Wiley-VCH Verlag GmbH, D-69469 (FRG) 1999; Chapter 3.9, p 150.

(4) Bussell, M. E.; Somorjai, G. A. *J. Catal.* **1987**, *106*, 93.

(5) Pecoraro, T.; Chianelli, R. R. *J. Catal.* **1981**, *67*, 430.

(6) Słoczynski, Jerzy. *J. Phys. Chem. B* **2002**, *106*, 7718.

(7) Ressler, T. *J. Phys. Chem. B* **2002**, *106*, 7719.

(8) Delporte, P.; Meunier, F.; Pham-Huu, C.; Vennegues, P.; Ledoux, M. J.; Guille, J. *Catal. Today* **1995**, *23*, 251.

(9) Bouchy, C.; Pham-Huu, C.; Heinrich, B.; Chaumont, C.; Ledoux, M. J. *J. Catal.* **2000**, *190*, 92.

(10) Bouchy, C.; Pham-Huu, C.; Ledoux, M. J. *J. Mol. Catal. A* **2000**, *162*, 317.

(11) Matsuda, T.; Kodama, H.; Sakagami, H.; Takahashi, N. *App. Catal. A* **2003**, *248*, 269.
(12) Matsuda, T.; Watanabe, K.; Sakagami, H.; Takahashi, N. *Appl. Catal. A* **2003**, *242*, 267.
(13) Sakagami, H.; Asano, Y.; Takahashi, N.; Matsuda, T. *Appl. Catal. A* **2005**, *284*, 123.
(14) Wang, D.; Su, D. S.; Schlögl, R. *Z. Anorg. Allg. Chem.* **2004**, *630*, 1007.
(15) Perdew, J. P.; Burke, K.; Ernzerhof, M. *Phys. Rev. Lett.* **1996**, *77*, 3865.
(16) Segall, M. D.; Lindan, P. L. D.; Probert, M. J.; Pickard, C. J.; Hasnip, P. J.; Clark, S. J.; Payne, M. C. *J. Phys.: Condens. Matter* **2002**, *11*, 2717.
(17) Bouchy, C.; Pham-huu, C.; Ledoux, M. J. *J. Mol. Catal. A* **2000**, *162*, 317.
(18) Alemán-Vazquéz, L. O.; Torres-García, E.; Villagómez-Ibarra, J. R.; Cano-Domínguez, J. L. *Catal. Lett.* **2005**, *100*, 219.
(19) Xiao, T.-c.; York, A. P. E.; Williams, V. C.; Al-Megren, H.; Hanif, A.; Zhou, X.-y.; Green, M. L. H. *Chem. Mater.* **2000**, *12*, 3896.
(20) Dufour, L. C.; Bertrand, O.; Floquet, N. *Surf. Sci.* **1984**, *147*, 396.
(21) Benadda, A.; Katrib, A.; Baramab, A. *Appl. Catal. A* **2003**, *251*, 93.
(22) (a) Wehrer, P.; Bigey, C.; Hilaire, L. *Appl. Catal. A* **2003**, *243*, 109. (b) Wehrer, P.; Hilaire, L.; Petit, E. *Appl. Catal. A* **2004**, *273*, 249.
(23) Lee, J. S.; Volpe, L.; Ribeiro, F. H.; Boudart, M. *J. Catal.* **1988**, *112*, 44.
(24) Yacamán, M. J.; Marin, M.; Ascencio, J. A. *J. Mol. Catal. A* **2001**, *173*, 61.
(25) Yacamán, M. J.; Ascencio, J. A.; Liu, H. *J. Vac. Sci. Technol. B* **2001**, *19*, 1091.
(26) Troiani, H. E.; Camacho-Bragado, G. A.; Miki-Yoshida, M.; Marquez, M. A. L.; Rubio, A.; Ascencio, J. A.; Jose-Yacaman, M. *Nanoletters* **2003**, *3*, 751.
(27) Aleman-Vázquez, L. O.; Torres-García, E.; Rodríguez-Gattorno, G.; Ocotlán-Flores, J.; Camacho-López, M. A.; Cano, J. L. *J. Solid State Chem.* **2004**, *177*, 3281.
(28) Dieterle, M.; Weinberg, G.; Mestl, G. *Phys. Chem. Chem. Phys.* **2002**, *4*, 812.
(29) Dieterle, M.; Mestl, G. *Phys. Chem. Chem. Phys.* **2002**, *4*, 822.
(30) Mestl, G.; Ruiz, P.; Delmon, B.; Knözinger, H. *J. Phys. Chem.* **1994**, *98*, 11269.
(31) Knight, D. S.; White, W. B. *J. Mater. Res.* **1989**, *4*, 365.
(32) Bartlett, B. F.; Tysoe, W. T. *Catal. Lett.* **1997**, *46*, 101.
(33) Nakamizo, M.; Kammereck, R.; Walker, P. L. *Carbon.* **1974**, *12*, 259.
(34) García-Santibañez, F.; Barragán-Vidal, A.; Gutiérrez, A.; Mendoza, M.; Ascencio, J. A. *Appl. Phys. A* **2000**, *71*, 219.
(35) Esparza, R.; Rosas, G.; Ascencio, J. A.; Pérez, R. *Mater. Sci. Eng. A* **2004**, *38*, 123.
(36) Ascencio, J. A.; Pérez, M.; Tehuacanero, S.; Yacamán, M. J. *Appl. Phys. A* **2001**, *73*, 295.
(37) Katrib, A.; Benadda, A.; Sobczak, J. W.; Maire, G. *Appl. Catal. A* **2003**, *242*, 31.
(38) Benadda, A.; Katrib, A.; Barama, A. *Appl. Catal. A* **2003**, *251*, 93.
(39) Egerton, R. F. *Electron Energy Loss Spectroscopy in the Electron Microscope*; Plenum Press: New York, 1986.
(40) Berhault, G.; Mehta, A.; Pavel, A. C.; Yang, J.; Rendon, L.; Yacamán, M. J.; Araiza, L. C. Moller, A. D.; Chianelli, R. R. *J. Catal.* **2001**, *198*, 9.